Measuring residual stress in finite thickness plates using the hole-drilling method

Marco Beghini[1], Leonardo Bertini[1], Anoj Giri[1] iD, Ciro Santus[1] and Emilio Valentini[2]

Abstract
Hole-drilling is one of the most popular methods for measuring residual stress in mechanical components. The ASTM E837 standard defines the hole-drilling method for plates that are either thicker or thinner than the size of the hole diameter and provides the related calibration coefficients for these two conditions. Measurements for components with a thickness in the range of a few millimetres, such as typical metal sheets, are not considered. In this article, the effects of thickness on the hole-drilling measurements are examined by a finite element parametric analysis. A method is proposed to analyse the measurements in plates with an intermediate thickness. The procedure is suitable for determining a general in-depth non-uniform residual stress distribution. Mathematical relationships are proposed which enable calibration coefficients to be obtained for any thickness. An experimental application confirms the validity of the procedure.

Introduction

Residual stresses are generally induced during the manufacturing of engineering components, and the magnitude and the stress orientation depend on the type of process, its parameters, and the material properties. The magnitude of the residual stresses can be comparable to the yield strength of the material, for instance in welds, and the effect of the residual stresses can be either beneficial or detrimental for the static and fatigue strength of the component.

Techniques for measuring the residual stresses are commonly classified into three categories: destructive, semi-destructive, and non-destructive.[1] Destructive or semi-destructive techniques require the material to be slit or removed. As the tractions due to the residual stresses are relaxed on the new surfaces created, a strain redistribution is produced in the body being investigated. The post-processing of the measured strains due to the relaxation is a typical inverse problem where the residual stress distribution is unknown.[2,3]

Hole-drilling is one of the most widely used semi-destructive methods. A small hole, with a typical diameter of $D_0 = 2\,mm$, is drilled on the surface of the component at the centre of a strain-gage rosette that is

used to measure the strains produced by the drilling.[4,5] If in-depth variations of the residual stress are expected, the hole must be performed in a sequence of steps and then the strains are measured at any increment (incremental hole-drilling). For this technique, the calibration coefficients necessary to apply the inverse calculation mainly depend on the geometry of the strain-gage rosette, the hole diameter, and their location in relation to each other.

In the common applications of the inverse procedure, the hypothesis of a linear elastic homogeneous and isotropic material during the drilling is accepted. In the ASTM E837-13:2013[5] standard, the calibration coefficients are collected in matrices for the configurations typically used. Initially, these calibration coefficients were evaluated experimentally; however, the finite element (FE) method has since been more

[1]Department of Civil and Industrial Engineering, University of Pisa, Pisa, Italy
[2]SINT Technology Srl, Florence, Italy

Corresponding author:
Anoj Giri, Department of Civil and Industrial Engineering, University of Pisa, Largo Lucio Lazzarino, 56122 Pisa, Italy.
Email: anoj.giri@ing.unipi.it

efficiently applied.[6,7] The integral method (IM) is one of the most common procedures used to numerically solve the inverse problem of deducing the residual stresses from the measured strains. In the IM, each residual stress component is assumed to be constant over each in-depth increment of the hole.

One limitation of the standard interpretation of hole-drilling is that the stress concentration, due to the introduction of the hole, produces a local plastic strain field if the residual stresses are sufficiently high. In the last few decades, some studies have demonstrated that the yielding near the hole affects the measurement if the residual stresses are above 60% of the material yield strength.[5,8–14] If the effect of plasticity is neglected and the influence coefficients evaluated in the linear-elastic hypothesis are used, residual stresses obtained by the IM are overestimated and leading to unacceptable results with values above the material yield strength.

The eccentricity between the hole and the rosette is another parameter that significantly affects the accuracy of the measurement.[15–20] Vangi[15] and Peral et al.[20] studied the effect produced by the eccentricity in the evaluation of non-uniform residual stresses. Beghini et al.[16,17] modelled the effect of the eccentricity by introducing dedicated influence functions.[16] Barsanti et al.[19] proposed a modified IM to reduce the error due to the eccentricity.

Research has also focused on improving the accuracy of the hole-drilling by considering other aspects such as the drilling step size optimization, the shape of the hole (in particular the geometry of the corner between the cylindrical region and the flat base), the effect of the Poisson ratio, and the influence of the drilling process parameters, for example, the rotational speed and the feed, on the hole geometry.[21–23] Peral et al.[24] performed an uncertainty analysis for non-uniform residual stress evaluation in incremental hole-drilling and demonstrated that the accuracy in the hole depth is the most significant parameter.

Generally, the hole-drilling method is used to measure the residual stress up to 1–1.5 mm depth with spatial resolution around 0.05 mm. To measure the residual stresses with a significantly finer depth resolutions than 0.05 mm (say micro and nano levels), researchers[25,26] have explored the FIB-DIC micro-hole-drilling and micro-ring-core techniques, for which any thickness size of the component is orders of magnitude larger than these milled depths.

Although from a physical point of view, the hole diameter D_0 should be the most significant characteristic length for scaling the geometry, it is common practice to assume the mean diameter of the rosette D as the characteristic length of the problem. This is due to the fact that the rosettes for hole-drilling are defined in the ASTM E837 standard and cannot be changed if influence coefficients provided by the standard are used. As a consequence of the drilling process, the hole has an effective diameter that can be measured only at the end.

The D_0 is accepted if $0.37 \leqslant D_0/D \leqslant 0.41$, that is, for the typical value $D = 5.13$ mm, 1.88 mm $\leqslant D_0 \leqslant 2.12$ mm.

Research on hole-drilling is usually aimed at components with a thickness t larger than the rosette mean diameter D (i.e. $t > D$). In these conditions (thick plates), the influence coefficients are independent of the thickness and they can be obtained by an FE model in which the hole is produced in a virtually semi-infinite body. If the plate thickness is much lower than the rosette mean diameter (for instance, $t \leqslant 0.2D$), the plane stress solution holds. In these conditions (thin plates), the in-depth residual stress gradient is neglected and the through-hole method is applied. The influence coefficients for the thin plates can be directly deduced by Kirsch's solution of a membrane with a circular hole.[27] However, in some applications, the component to be measured has a thickness that is somewhere between thin and thick. For this intermediate case, the plate thickness t becomes a new parameter affecting the influence coefficients of the incremental hole-drilling.

A few researchers have examined the residual stress measurement for a plate with an intermediate (or finite) thickness.[28–30] Schajer and Abraham[28] proposed a procedure to evaluate the most appropriate calibration coefficients for measuring uniform in-depth residual stress fields. Schuster et al.[30] considered the effects of plasticity in components with a thickness in the range of 1 mm $< t <$ 4 mm.

To the best of the authors' knowledge, a complete procedure for obtaining the residual stress in components with an intermediate thickness, affected by a general not uniform in-depth residual stress, has not yet been developed. The aim of this article is thus to fill this gap. The influence coefficients for the IM were determined by a parametric FE analysis performed with several t/D ratios for the most commonly employed strain-gage rosettes. Interpolation functions were then obtained for calculating the influence coefficients for any t/D ratio. A complete procedure is proposed by which general in-depth non-uniform residual stress can be obtained for an intermediate thickness. An experimental validation was carried out by applying the procedure in specimens with a thickness of 1.6 and 6 mm ($t/D = 0.31$ and 1.17, respectively).

Problem definition and formulation

When the thickness t is much less than the hole diameter (thin conditions), the residual stress gradient in the thickness direction is usually neglected and a through hole is generally produced in a single step. However, the thickness is most commonly much larger than the hole diameter (thick conditions) and the residual stress gradients are generally expected in the in-depth direction. The ASTM-E837 standard considers either uniform in-depth residual stresses for thin plates or uniform and non-uniform residual stress in the case of thick plates. There is no procedure for determining

Figure 1. Hole-drilling specification of the ASTM E837 for the commonly used strain-gage rosettes with a gage diameter $D = 5.13$ mm.

non-uniform residual stresses for plates with an intermediate thickness. By assuming the standard strain-gage rosettes A and B type with a mean diameter $D = 5.13$ mm, the typical hole diameter is $D_0 = 2$ mm, and the range of the intermediate plate thickness, not covered by the standard, is 1.0 mm $< t < 5.2$ mm.[5] Figure 1 provides an overview of the hole-drilling specifications.

The following equation relates the residual stress components and the strain measured by a strain-gage with the grid radially oriented around the centre of the hole

$$\varepsilon(\theta) = \frac{(1 + \nu)\,\bar{a}\,(\sigma_X + \sigma_Y)}{E} + \frac{\bar{b}\,(\sigma_X - \sigma_Y)}{E}\cos(2\theta) \tag{1}$$

where E and ν are Young's modulus and Poisson's ratio, respectively; X and Y are the directions of the in-plane principal residual stresses σ_X and σ_Y; θ is the counter-clockwise angle from the X-direction of the grid direction; and $\bar{a}, \bar{b}$ are the influence coefficients. For through holes in thin plates, $\bar{a}, \bar{b}$ are two scalars that can be evaluated by integrating the strain obtained by Kirsch's solution. When applying incremental hole-drilling, an equation of type (1) holds for any in-depth hole increment; therefore, $\bar{a}, \bar{b}$ are matrices of influence coefficients, and these matrices are determined by FE simulations. For thick and thin plates, these influence coefficient matrices are provided by the ASTM-E837 standard.

In incremental hole-drilling, the hole is performed in a sequence of n partial depths h_i, each indicated by the subscript i ($i = 1, 2, 3, \ldots, n$) with $h_0 = 0$. When the IM is applied for solving the inverse problem, each component of the residual stress is modelled by a sequence of stresses that are assumed to be constant within each depth increment $h_j - h_{j-1}$. The strains measured by the three strain-gages of the rosette $(\varepsilon_1, \varepsilon_2, \varepsilon_3)_i$ are measured and recorded for each partial hole depth h_i (Figure 2).

The residual stress components usually refer to the system of axis defined by the rosette with the (lower case) x axis in the direction of the strain-gage 1 and the (lower case) y axis in the direction of the strain-gage 3.

In general, the system x-y is not principal for the residual stress and, as a consequence, three residual stress components are expected for any hole depth increment: two normal σ_x and σ_y, and one shear τ_{xy} component. For each partial hole increment i (with $j \leqslant i$), the following relationships (2)–(4) hold

$$p_i = \frac{(\varepsilon_3 + \varepsilon_1)_i}{2}, \quad q_i = \frac{(\varepsilon_3 - \varepsilon_1)_i}{2},$$

$$t_i = \frac{(2\varepsilon_2 - \varepsilon_3 - \varepsilon_1)_i}{2} \tag{2}$$

$$P_j = \frac{\left[(\sigma_y)_j + (\sigma_x)_j\right]}{2}, \quad Q_j = \frac{\left[(\sigma_y)_j - (\sigma_x)_j\right]}{2},$$

$$T_j = (\tau_{xy})_j \tag{3}$$

$$\bar{a}\vec{P} = \frac{-E\vec{p}}{(1 + \nu)}, \quad \bar{b}\vec{Q} = -E\vec{q}, \quad \bar{b}\vec{T} = -E\vec{t} \tag{4}$$

where the over-barred symbols represent $n \times n$ matrices, and the arrowed symbols are column vectors (or $n \times 1$ arrays). After rearranging equation (3), the residual stress components in the region between h_{j-1} and h_j can be determined as follows

$$(\sigma_x)_j = P_j - Q_j, \quad (\sigma_y)_j = P_j + Q_j, \quad (\tau_{xy})_j = T_j \tag{5}$$

In equation (4), $\bar{a}, \bar{b}$ are lower triangular matrices. For example, with three hole steps ($n = 3$), the matrices are represented as

$$\bar{a} = \begin{bmatrix} a_{11} & 0 & 0 \\ a_{21} & a_{22} & 0 \\ a_{31} & a_{32} & a_{33} \end{bmatrix}, \quad \bar{b} = \begin{bmatrix} b_{11} & 0 & 0 \\ b_{21} & b_{22} & 0 \\ b_{31} & b_{32} & b_{33} \end{bmatrix} \tag{6}$$
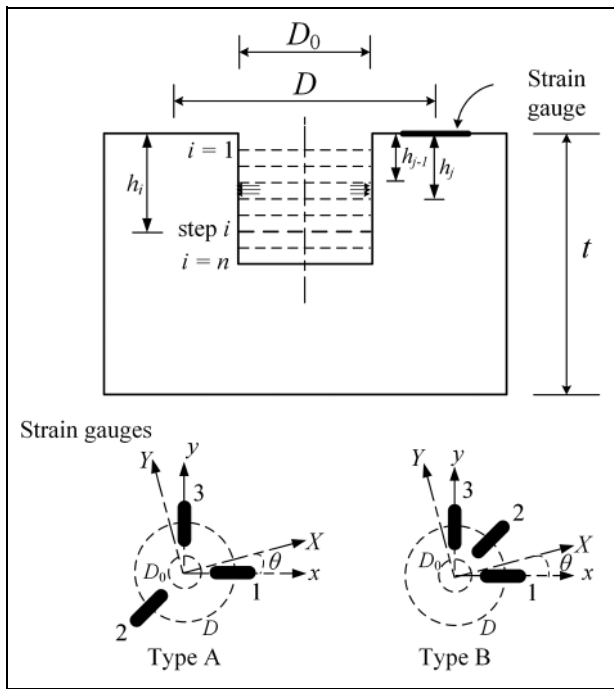
Figure 2. Drilling sequence and strain-gage positions for type A and type B rosettes. Plane axes with general (not principal) *x* and *y* directions.
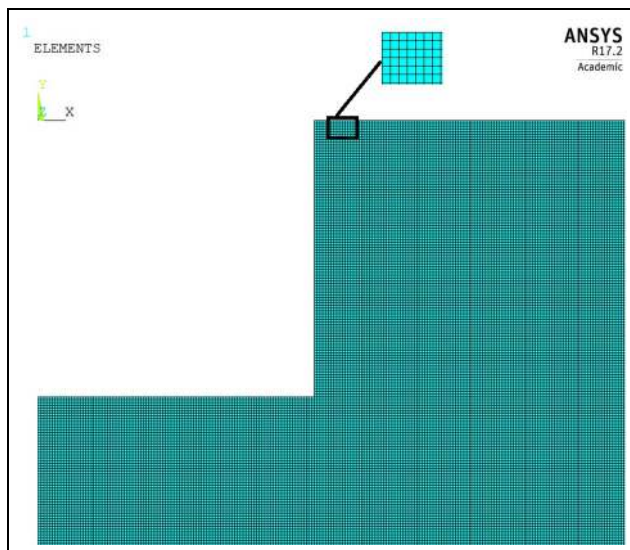
Figure 3. 2D FE model for *t*/*D* = 0.3.

FE analyses

In the FE simulations of the measurement, the material was assumed to be homogeneous isotropic linear elastic with $E = 200$ GPa and $\nu = 0.3$. Figure 3 shows the two-dimensional (2D) FE model with an enlarged view of the meshing at the hole boundary. The dimension of the elements in this region was kept as small as $0.002\,D$. In order to cover the range from the intermediate thickness to the thick conditions, 18 values of the thickness *t* were considered: $t/D = 0.2, 0.22, 0.24, 0.25, 0.275, 0.3,$ 0.33, 0.36, 0.4, 0.44, 0.48, 0.6, 0.66, 0.72, 1, 1.1, 1.2, and 3.0.

The quantity $(\sigma_X + \sigma_Y)/2$ in equation (1) represents equi-biaxial residual stress and the $\bar{a}$ matrix was evaluated by means of 2D axi-symmetric FE models.[28] Conversely, the term $(\sigma_X - \sigma_Y)/2$ in equation (1) shows a $\cos(2\theta)$ angular dependence[16,28] and the associated strains have $\sin(2\theta)$ and $\cos(2\theta)$ dependence.[31,32] As a consequence, the same 2D FE mesh was used to determine the $\bar{b}$ matrix as well, but Fourier or axi-harmonic elements (PLANE 25 in ANSYS) were employed.

The removal of the material in the presence of residual stresses was numerically simulated by applying the opposite relaxed tractions at the hole surface. The shear components were simulated by superimposing a distribution of normal tractions to a distribution of tangential tractions with a relative phase equal to 45°. For any hole depth h_i, in-depth uniform tractions were applied in the region starting from the surface to any partial hole depth h_j ($j \leqslant i$) and then operating a difference, in terms of the deformation field, with the load up to h_{j-1}.

The strain-gage responses were calculated as the mean value of the extensional strain in the direction of the gage grid on the region of the gage. This quantity was computed as the difference of the mean values of the displacements (in the grid direction) of the external and internal sides of the gage, divided by the gage length. Using the relations in equations (2)–(4), the calibration matrixes were determined as the strain-gage responses corresponding to unit applied pressures, and this calculation was repeated for each plate thickness examined.

The coefficients were obtained for the Type A rosette (gage length and gage width GL = GW = 1.57 mm and average gage diameter $D = 5.13$ mm) and Type B rosette (gage length GL = 1.57 mm, gage width GW = 1.14 mm and $D = 5.13$ mm) in accordance with the ASTM-E837 standard. For each t/D ratio considered, the matrices of the influence coefficients were then calculated for three different hole diameters: 1.8, 1.9, and 2 mm.

The maximum hole depth ($h_{\max} = h_n$) was kept at 1.0 mm for each plate thickness and hole diameter in accordance with the ASTM-E837 standard. The number of hole increments was $n = 20$; therefore, the numerically simulated hole depth increment ($h_i - h_{i-1}$) was 0.05 mm. A total number of 108 FE simulations were performed and 45,360 influence coefficients were calculated.

Results and discussion

Effect of the plate thickness on the influence coefficients

Due to the huge number of results obtained, it is not feasible to show how each influence coefficient depends on the parameters of the problem. A few coefficients were therefore selected in order to discuss the typical
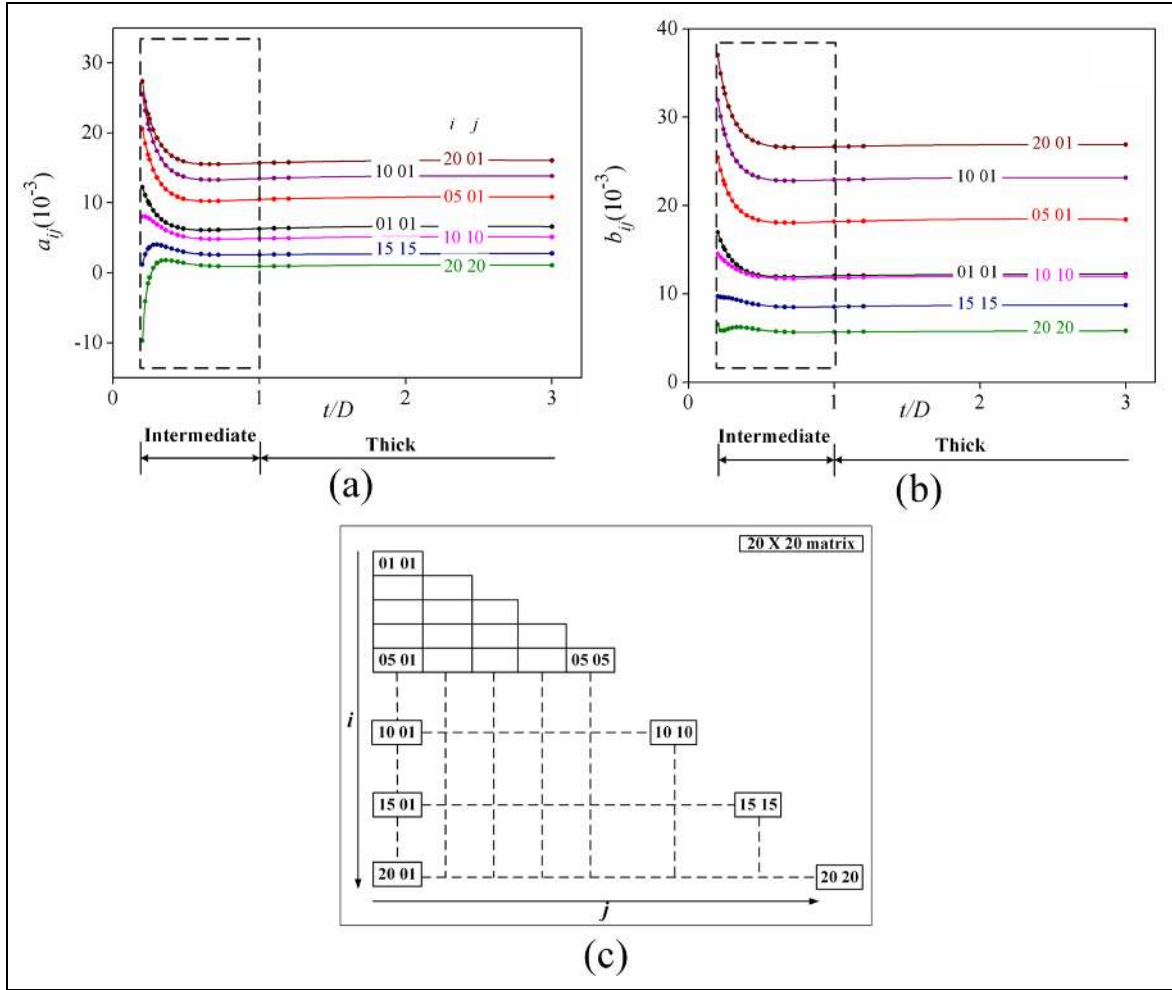
Figure 4. Calibration coefficients as a function of the plate thickness: (a) for a_{ij} and (b) for b_{ij}, and (c) position of the coefficients in the matrices and definition of i and j subscripts.

trends observed. Figure 4 shows the effect of the plate thickness on a few coefficients a_{ij} and b_{ij} for the Type A rosette with $D_0 = 2$ mm.

As expected, the coefficients did not vary significantly and assumed the asymptotical value of the thick condition when $t/D > 1$. Conversely, a strong dependence on the plate thickness was observed in the intermediate conditions. This behaviour is the consequence of the reduced constraint, due to the free surface below the hole, and is more evident in the thinner plates. A similar high sensitivity of the influence coefficient values for thin plates was also observed by Schajer and Abraham[28] under the condition of in-depth uniform residual stress.

As shown in Figure 4(a), in the intermediate thickness region, some a_{ij} coefficients show a positive gradient, while others show a negative gradient, and the variations are mostly confined at the very initial region of the intermediate thickness range. Some of these coefficients, for instance $a_{20\ 20}$, experience a sign change and are positive for large thicknesses and negative for small thickness values. Conversely, the coefficients b_{ij} are always positive and mostly with a negative gradient

at the initial region of the intermediate thickness range, Figure 4(b).

In order to provide an operative procedure for the practical application, the calibration coefficients need to be evaluated for the effective thickness. Thus, analytical relationships were found by interpolating the numerical results. As evident in Figure 4, not all the numerically obtained coefficients have a monotonic dependence on the thickness (see, for instance, $a_{15\ 15}$ and $a_{20\ 20}$). As a consequence, having selected a sum of exponentials in order to model the coefficient functions, more than one exponential term was necessary to accurately capture these trends.

The following equations (7) and (8) were found to adequately reproduce the observed thickness dependences of all the coefficients

$$a_{ij} = \alpha_{1,ij}e^{-20\omega} + \alpha_{2,ij}e^{-15\omega} + \alpha_{3,ij}e^{-8\omega}$$
$$+ \alpha_{4,ij}e^{-2.5\omega} + \alpha_{5,ij} \tag{7}$$

$$b_{ij} = \beta_{1,ij}e^{-20\omega} + \beta_{2,ij}e^{-15\omega} + \beta_{3,ij}e^{-8\omega}$$
$$+ \beta_{4,ij}e^{-2.5\omega} + \beta_{5,ij} \tag{8}$$
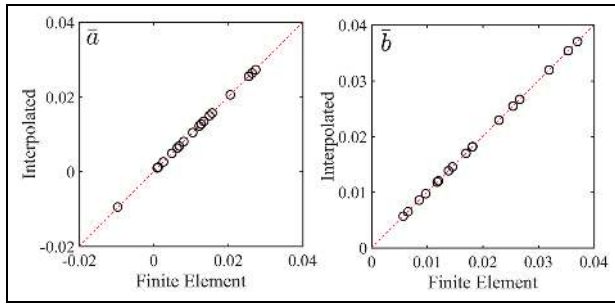
Figure 5. Influence coefficients obtained by the interpolating equations (7) and (8) plotted versus the FE values for $t/D = 0.2$ and $t/D = 1$.

where $\omega = t/D$ is the dimensionless thickness.

When the thickness is sufficiently high, all the (negative) exponential terms vanish and only the constant terms $\alpha_{5,ij}$ and $\beta_{5,ij}$ remain. They were thus set as equal to the calibration coefficients for the thick plate. The complete set of the constants $\alpha_{k,ij}$ and $\beta_{k,ij}$ (with $k = 1, \ldots, 5$) obtained by least square interpolations of the numerically evaluated coefficients are reported in Supplemental Appendix for both the examined rosettes with the reference hole diameter $D_0 = 2.0$ mm.

For almost all the coefficients, the correlation R^2 of the numerical result interpolations was above 0.99 and only for a few coefficients of the $\bar{b}$ matrix, the worst condition with $R^2 = 0.97$ was found. The adequacy of the proposed relationships (7) and (8) can be verified by the correlation plots in Figure 5 in which the results for the same coefficients reported in Figure 4 were plotted considering $t/D = 0.2$ and $t/D = 1$.

Effect of the hole diameter

The influence coefficients were evaluated for three hole diameters: 1.8 mm, 1.9 mm and 2.0 mm, which are close to the usually measured hole values. However, for the sake of simplicity, only the results for the nominal value $D_0 = 2.0$ mm are reported in Supplemental Appendix. A method for also considering the effective hole diameter is reported hereafter.

The ASTM-E837 states that the measured strains are (approximately) proportional to the area of the hole or, equivalently, to the square of the hole diameter. As the calibration coefficients are directly related to the measured strain components p and q, as reported in equation (4), it can be concluded that they should also be proportional to the area of the hole. In order to verify this assumption, the ratios $\rho_{a,ij}$, defined in equation (9), were evaluated

$$\rho_{a,ij} = \frac{a_{ij,d0}/a_{ij,D0}}{d_0^2/D_0^2} \tag{9}$$

where $d_0 = 1.8$ or 1.9 mm, $a_{ij,d0}$ is the a_{ij} coefficient for the hole diameter d_0, and the $a_{ij,d0}$ is the a_{ij} coefficient for the reference hole diameter $D_0 = 2$ mm. Similarly, $\rho_{b,ij}$ ratios were defined for the matrix $\bar{b}$ coefficients. All

the ρ ratios should be equal to 1 if the aforementioned hypotheses were correct.

Figure 6 plots the ratios $\rho_{a,ij}$ and $\rho_{b,ij}$ for the first and last coefficients of the matrix, for the type A rosette. The ρ ratios for the coefficients $a_{01\ 01}$ and $b_{01\ 01}$ are within the range $\pm 5\%$ and $\pm 1\%$, respectively, of the expected unit value for all the t/D ratios analysed. The maximum deviations from the unit were 1.17 and 1.16 for ratios $\rho_{a,20\ 20}$ and $\rho_{b,20\ 20}$, respectively. For the coefficient $a_{20\ 20}$, the ρ ratio increases with the thickness t/D and becomes constant when $t/D > 1.2$. For $t/D > 0.6$, a few coefficients of the $\bar{a}$ matrix (in the bottom right corner) have ρ ratios that differ by 10% from the unit for the hole diameter $d_0 = 1.8$ mm. For the coefficient $b_{20\ 20}$, the maximum ρ ratio was found at the lowest thickness and decreases sharply becoming constant as t/D increases. The ρ ratios for the $\bar{b}$ matrix generally differ from the unit by no more than 5% for almost all the coefficients, irrespectively of the plate thickness and the hole diameter, except for a few coefficients (near the bottom right-hand corner of the matrices) with ρ ratios differing from the unit by no more than 10%.

It can be concluded that the influence coefficients are not exactly proportional to the area of the hole. However, the error introduced by this hypothesis can be estimated in the order of a few percent, if the effective hole diameter differs by no more than 10% from the nominal value. As a consequence, the proportionality to the area of the hole can be considered as a reasonable hypothesis that can be applied in the absence of specific calibration coefficients for any practical application.

Procedure for evaluating residual stress in the intermediate regime

Assuming the hypothesis suggested by the ASTM E837 standard with regard to the effective hole diameter, the coefficients reported in Supplemental Appendix can be used to evaluate the residual stress in a plate of any thickness.

The procedure for measuring residual stress is as follows:

(a) *Range of application.* Rosette type A or type B with $D = 5.13$ mm, plate thickness $t \geq 1.03$ mm, effective measured hole diameter 1.8 mm $\leq d_0 \leq 2.0$ mm.

(b) *Test execution.* Apply the incremental hole-drilling in accordance with the ASTM-E837 standard with 0.05-mm steps.

(c) *Evaluation of matrices $\bar{a}$ and $\bar{b}$ for the effective thickness.* First, the calibration coefficients need to be determined for the reference hole diameter ($D_0 = 2$ mm) with equations (7) and (8). After this, the corrected matrices $\bar{a}$ and $\bar{b}$ for the measured hole diameter can be determined by inverting equation (9) and just assuming unit ρ ratios. The example of calculation for calibration coefficients are shown in Appendix 2.
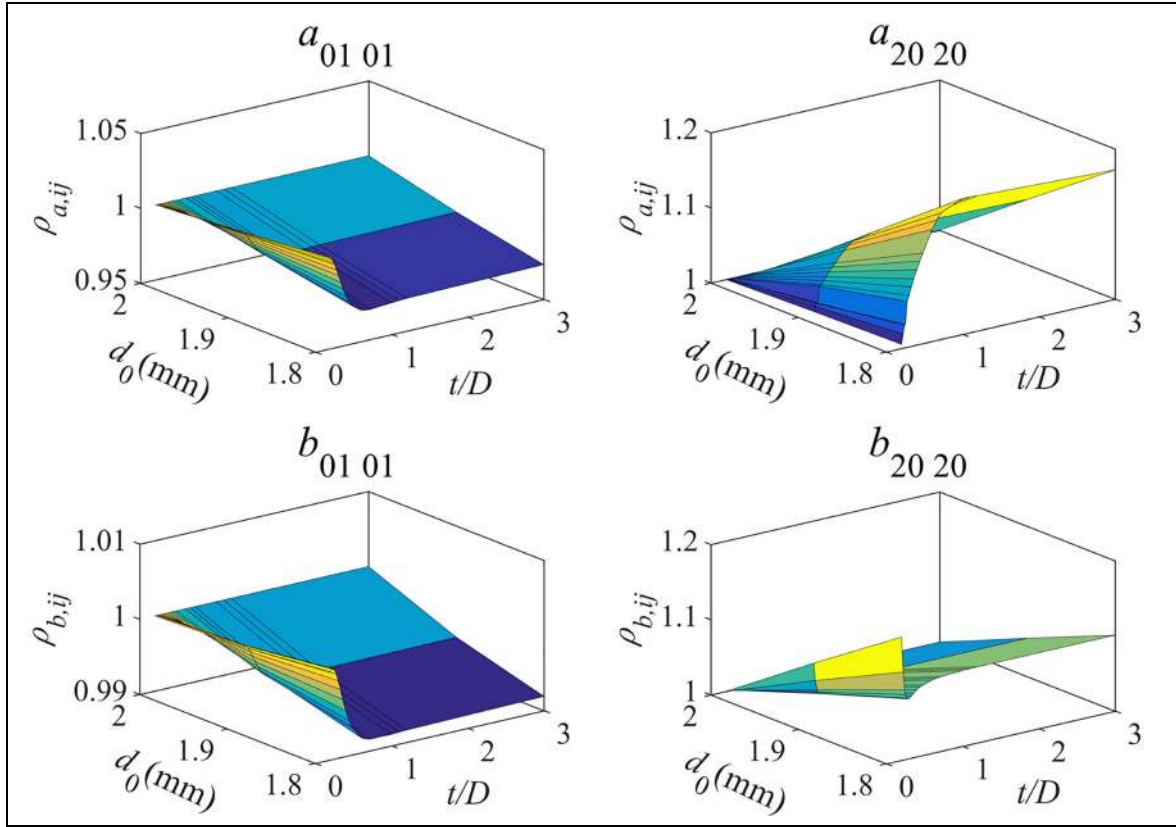
Figure 6. Surface plots of the effective diameter ratios ρ.

(d) *Evaluation of the residual stress distribution.* Apply the integral method according to the ASTM-E837 standard with the obtained matrices $\bar{a}$ and $\bar{b}$.

Experimental verification

In order to provide experimental verification of the proposed procedure, two specimens were designed and tested. The material was aluminium 2024-T351 with $E = 72$ GPa, $\nu = 0.3$, and yield strength $S_y = 300 \pm 5$ MPa. Specimen 1 (thick specimen) had a thickness of $t_1 = 6$ mm, whereas specimen 2 (thin specimen) had a thickness of $t_2 = 1.6$ mm in the intermediate region.

As shown in Figure 7, on each specimen, three strain-gage rosettes of type CEA-06-062UM-120 were placed with the y axis (grid 3) along the longitudinal direction. For each rosette, different hole depths were drilled: 0.2, 0.5, and 1.0 mm. Figure 7(a) and (b) shows the thick specimen before and after drilling the holes. On the thin specimen, shown in Figure 7(c), three additional strain-gages were attached near the rosettes in order to independently measure the induced strain during the loading.

The residual stress was simulated by applying a tensile uniform uniaxial stress to the specimens using a standard tensile testing machine. Axial loads were applied with an intensity of 20 kN for the thick specimen and 7.27 kN for the thin specimen. With these values, both the specimens in the measured region were under the same conditions of uniform nominal stress $\sigma_0 = 152$ MPa.

For both specimens, the strains of all the rosette grids were measured before and then after drilling the holes with the load applied, after tare balancing the strains without the load. The relaxed strains that the rosettes would have measured if the holes had been performed under the load were obtained as the difference between the measurements without the hole and with the hole. Table 1 reports the measured relaxed strains, and the effect of the specimen thickness on the measurements is evident.

According to the procedure reported in section 'Procedure for evaluating residual stress in the intermediate regime', the matrices were initially determined for the nominal hole diameter $D_0 = 2$ mm using equations (7) and (8). The coefficients were then corrected using equation (9) to consider the effective hole diameters d_0, which were measured after the drilling and are reported in Table 2.
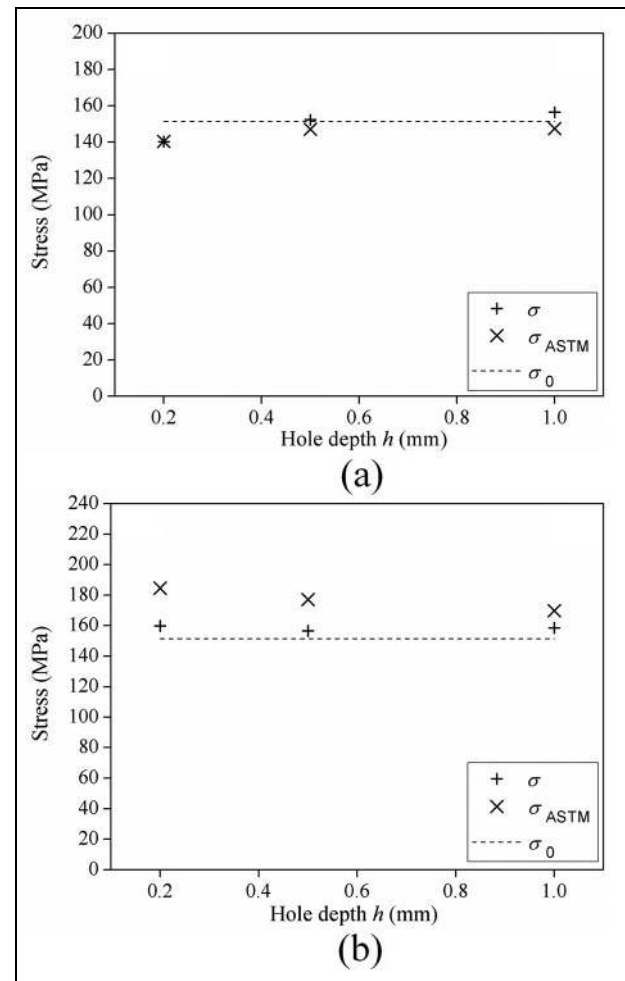
The calibration coefficients for the effective hole diameter, hole depth, and plate thickness were calculated. The residual stresses determined from the measured strains are shown in Figure 8(a) and (b). Only the axial stress components are reported as the others were verified to be negligible. The values calculated by the proposed procedure are indicated with σ, while the values obtained by the ASTM-E837 standard (neglecting the thickness effect) are indicated as σ_{ASTM}. The dashed line represents the reference stress σ_0 (applied value).

For the thick specimen, Figure 8(a), the stresses calculated by the proposed procedure were in agreement
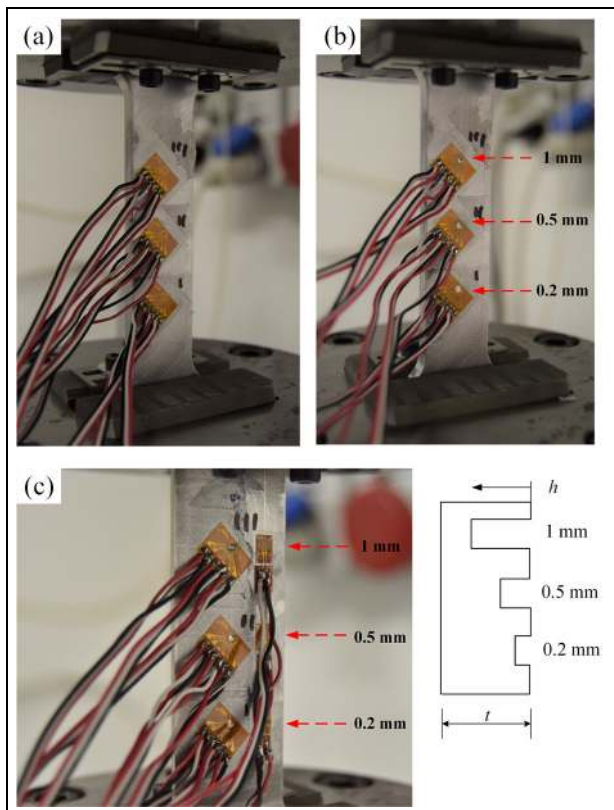
Figure 7. Test specimens on the testing machine with strain-gage rosettes: (a) thick specimen before drilling the holes, (b) thick specimen after drilling the holes and (c) thin specimen after drilling the holes.

Figure 8. Stresses in (a) thick specimen $t_1 = 6$ mm and (b) thin specimen $t_2 = 1.6$ mm.

with the values obtained by the ASTM E837-13 standard (maximum relative difference 5%). For the thin specimen, Figure 8(b), the stresses calculated by the ASTM standard overestimated the applied value by about 20%, thus indicating that, as expected, the specimen thickness is in the intermediate region. The stress evaluated for the hole depth of 0.2 mm and with the proposed procedure was 160 MPa, which was higher (about 6%) than the applied stress. For the hole depths

of 0.5 and 1 mm, the differences between the stress evaluated by the procedure and the nominal value were lower. In any case, the results obtained with the proposed procedure were affected by the same order of error as the thick specimen.

Table 1. Measured relaxed strains (10^{-6}).

Hole depth (h)	0.2 mm		0.5 mm		1.0 mm	
Thickness (t)	1.6 mm	6 mm	1.6 mm	6 mm	1.6 mm	6 mm
ε_1 (Transverse direction)	17	−18	25	66	132	141
ε_2	−60	−56	−140	−105	−263	−175
ε_3 (Loading direction)	−114	−86	−344	−281	−583	−510

Table 2. Measured hole diameters d_0 (mm).

Hole depth (h)	0.2 mm	0.5 mm	1 mm
Thick specimen $t_1 = 6.0$ mm	1.78	1.74	1.74
Thin specimen $t_2 = 1.6$ mm	1.73	1.79	1.75

Table 3. Calculated stresses for thin specimen (MPa).

Hole depth (h)	0.2 mm	0.5 mm	1.0 mm
σ_0 (Longitudinal)	152	152	152
σ (Longitudinal)	159.9	156.6	158.5
σ_{ASTM} (Longitudinal)	184.5	177.6	169.8
σ (Transverse)	−5.5	9.2	−3.0
σ_{ASTM} (Transverse)	9.9	26.1	8.4

Since the applied loading is uniaxial tensile, it is assumed that the stress in the other direction (transverse) is zero. To confirm this, the values of the orthogonal stress component were also calculated according to the proposed procedure. Table 3 shows the obtained transverse residual stresses measured on the thin specimen. The stresses σ (Transverse) were found within the range of $\pm 6\%$, thus it can be concluded that this stress is in general not exactly zero, but it can be assumed negligible as compared with the applied stress.

The difference between the applied and measured stress in longitudinal direction (less than 6%) may be due to the small bending effect that was observed when testing the thin specimen. In addition, there was a small eccentricity between the rosette and the hole (although this was within the range indicated by the ASTM standard for the validity of the test) whose effect was not considered in the analysis.

Although preliminary and partial, these tests were considered a verification and provide an example of the practical applicability of the proposed procedure for obtaining hole-drilling residual stresses in plates with a finite thickness.

Conclusion

Using an extensive FE parametrical analysis, the calibration coefficients of the IM for measuring residual stress by incremental hole-drilling were found to be significantly influenced by the plate thickness if the thickness itself is similar or smaller than the hole diameter. If the coefficients proposed by the ASTM-E837 standard for thick plates are used when interpreting the measurements performed on a plate with a thickness of a few millimetres, systematic errors in the order of tens of percent can occur. The proposed procedure takes into account the effective thickness and produces estimates with a similar accuracy to that obtained in the commonly adopted hole-drilling method. The procedure can be applied in components affected by a general in-depth non-uniform residual stress. In order to facilitate the practical application of the procedure, continuous expressions were proposed by which the calibration coefficients can be directly evaluated for the effective thickness of the plate and the diameter of the produced hole. An experimental verification provided preliminary proof of the validity and accuracy of the procedure.

ORCID iD

Anoj Giri https://orcid.org/0000-0002-3216-0821

Supplemental material

Supplemental material for this article is available online.

References

1. Rossini NS, Dassisti M, Benyounis KY, et al. Methods of measuring residual stresses in components. *Mater Des* 2012; 35: 572–588.
2. Schajer GS. Hole-drilling residual stress measurements at 75: origins, advances, opportunities. *Exp Mech* 2010; 50: 245–253.
3. Schajer GS and Prime MB. Use of inverse solutions for residual stress measurements. *J Eng Mater Technol* 2006; 128: 375–382.
4. Withers PJ and Bhadeshia HKDH. Residual stress part 1 – measurement techniques. *Mater Sci Technol* 2001; 17: 355–365.
5. ASTM E837-13:2013. Standard test method for determining residual stresses by the hole-drilling strain gage method.
6. Schajer GS. Application of finite element calculations to residual stress measurements. *J Eng Mater Technol* 1981; 103(2): 157–163.
7. Schajer GS. Measurement of non-uniform residual stresses using the hole-drilling method. *J Eng Mater Technol* 1988; 110(4): 338–349.
8. Beghini M, Bertini L and Raffaelli P. Numerical analysis of plasticity effect in the hole-drilling residual stress measurement. *J Test Eval* 1994; 22(6): 522–529.
9. Lin YC and Chou CP. Error induced by local yielding around hole in hole drilling method for measuring residual stress of materials. *Mater Sci Technol* 1995; 1: 600–604.
10. Vangi D and Tellini S. Hole-drilling strain-gauge method: residual stress measurement with plasticity effects. *J Eng Mater Technol* 2010; 132: 1–7.
11. Beghini M, Bertini L and Santus C. A procedure for evaluating high residual stresses using the blind hole drilling method including the effect of plasticity. *J Strain Anal Eng* 2010; 45(4): 301–318.
12. Seifi R and Majd DS. Effects of plasticity on residual stresses measurement by hole drilling method. *Mech Mater* 2012; 53: 72–79.

13. Giri A, Pandey C, Mahapatra MM, et al. On the estimation of error in measuring the residual stress by strain gauge rosette. *Measurement* 2015; 65: 41–49.

14. Chupakhin S, Kashaev N, Klusemann B, et al. Artificial neural network for correction of effects of plasticity in equibiaxial residual stress profiles measured by hole drilling. *J Strain Anal Eng* 2017; 5(23): 137–151.

15. Vangi D. Residual stress evaluation by the hole-drilling method with off-center hole: an extension of the integral method. *J Eng Mater Technol* 1997; 119: 79–85.

16. Beghini M, Bertini L and Mori LF. Evaluating non-uniform residual stress by the hole-drilling method with concentric and eccentric holes. Part I: definition and validation of the influence functions. *Strain* 2010; 46: 324–336.

17. Beghini M, Bertini L and Mori LF. Evaluating non-uniform residual stress by the hole-drilling method with concentric and eccentric holes. Part II: application of the influence functions to the inverse problem. *Strain* 2010; 46: 337–346.

18. Nau A and Scholtes B. Experimental and numerical strategies to consider hole eccentricity for residual stress measurement with the hole drilling method. *Mater Test* 2012; 54: 296–303.

19. Barsanti M, Beghini M, Bertini L, et al. First-order correction to counter the effect of eccentricity on the hole-drilling integral method with strain-gage rosettes. *J Strain Anal Eng* 2016; 51(6): 431–443.

20. Peral D, Correa C, Diaz M, et al. Measured strains correction for eccentric holes in the determination of non-uniform residual stresses by the hole drilling strain gauge method. *Mater Des* 2017; 132: 302–313.

21. Stefanescu D, Truman CE, Smith DJ, et al. Improvements in residual stress measurement by the incremental centre hole drilling technique. *Exp Mech* 2006; 46: 417–427.

22. Nau A, Mirbach D and Scholtes B. Improved calibration coefficients for the hole-drilling method considering the influence of the Poisson ratio. *Exp Mech* 2013; 53: 1371–1381.

23. Blödorn R, Viotti MR, Schroeter RB, et al. Analysis of blind-holes applied in the hole-drilling method for residual stress measurements. *Exp Mech* 2015; 55: 1745–1756.

24. Peral D, Vicente J, Porro JA, et al. Uncertainty analysis for non-uniform residual stresses determined by the hole drilling strain gauge method. *Measurement* 2017; 97: 51–63.

25. Lunt ADJ and Korsunsky AM. A review of micro-scale focused ion beam milling and digital image correlation analysis for residual stress evaluation and error estimation. *Surf Coat Technol* 2015; 283: 373–388.

26. Korsunsky AM, Salvati E, Lunt ADJ, et al. Nanoscale residual stress depth profiling by focused ion beam milling and eigenstrain analysis. *Mater Des* 2018; 145: 55–64.

27. Timoshenko SP and Goodier N. *Theory of elasticity*. 3rd ed. New York: McGraw-Hill, 1970.

28. Schajer GS and Abraham C. Residual stress measurements in finite-thickness materials by hole-drilling. *Exp Mech* 2014; 54: 1515–1522.

29. Serra Y, Ficquet X and Kingston E. Residual stress measurement using the hole drilling technique on components outside the ASTM E837 standard. *Adv Mater Res* 2014; 996: 301–306.

30. Schuster S, Steinzig M and Gibmeier J. Incremental hole drilling for residual stress analysis of thin walled components with regard to plasticity effects. *Exp Mech* 2017; 57: 1457–1467.

31. Wilson EL. Structural analysis of axisymmetric solids. *AIAA J* 1965; 3(12): 2269–2274.

32. Zienkiewicz OC and Taylor RL. *The finite element method*. 6th ed. Oxford: Elsevier, 2005.

Appendix 1

Notation

$\bar{a}, \bar{b}$	lower triangular matrices of calibration coefficients
a_{ij}, b_{ij}	calibration coefficients for hole depth h_i with partial hole depth h_j
$a_{ij,d0}, b_{ij,d0}$	calibration coefficients a_{ij}, b_{ij} for the effective hole diameter d_0
$a_{ij,D0}, b_{ij,D0}$	calibration coefficients a_{ij}, b_{ij} for the reference hole diameter ($D_0 = 2$ mm)
D_0, d_0	reference hole diameter and effective (actual) hole diameter, respectively
D	Rosette mean diameter
E, ν	Young's modulus and Poisson's ratio
GL, GW	strain-gage grid length and width
h_i	partial hole depth ($i = 1, \ldots, n$ and $h_0 = 0$)
i, j	Indexes: $i = 1, \ldots, n$ and $j = 1, \ldots, i$ for the numerically simulated partial hole depths ($n = 20$) and for the components of the calibration matrices
t	plate thickness
$\alpha_{k,ij}$	fitting coefficients for obtaining $a_{ij,D0}$ ($k = 1, \ldots, 5$)
$\beta_{k,ij}$	fitting coefficients for obtaining $b_{ij,D0}$ ($k = 1, \ldots, 5$)
$\varepsilon_1, \varepsilon_2, \varepsilon_3$	measured strains for grids 1, 2, and 3, respectively
$\rho_{a,ij}$	effective hole diameter ratio for obtaining $a_{ij,d0}$ given $a_{ij,D0}$
$\rho_{b,ij}$	effective hole diameter ratio for obtaining $b_{ij,d0}$ given $b_{ij,D0}$
σ_0	stress applied during the tests
σ	stress evaluated in the tests by the proposed procedure
σ_{ASTM}	stress evaluated in the tests by the ASTM E837 standard (for thick plates)

Appendix 2

Example of the calculation of the calibration coefficients

The calculation of the calibration coefficients for type B rosette, plate thickness $t = 1.6$ mm, measured hole diameter $d_0 = 1.79$ mm, and hole depth $h = 0.5$ mm is reported in this appendix as an application example.

The dimensionless thickness is

$$\omega = t/D = 1.6/5.13 = 0.31$$

and the final hole depth is $h_i = 0.5\,\text{mm}$ $(i = 10)$. Therefore, by assuming that the residual stress is uniform up to this depth, the necessary coefficients of the matrix $\bar{a}$ are: $a_{10\ 01}, a_{10\ 02}, a_{10\ 03}, \ldots, a_{10\ 10}$ and similarly the coefficients of $\bar{b}$. Initially, the calibration coefficients are determined with equations (7) and (8) for a nominal hole diameter $D_0 = 2\,\text{mm}$

$$a_{ij} = \alpha_{1,ij}e^{-20\omega} + \alpha_{2,ij}e^{-15\omega} + \alpha_{3,ij}e^{-8\omega}$$
$$+ \alpha_{4,ij}e^{-2.5\omega} + \alpha_{5,ij}$$
$$b_{ij} = \beta_{1,ij}e^{-20\omega} + \beta_{2,ij}e^{-15\omega} + \beta_{3,ij}e^{-8\omega}$$
$$+ \beta_{4,ij}e^{-2.5\omega} + \beta_{5,ij}$$

From Supplemental Appendix, Tables 11–15 for type B rosette, the coefficients $\alpha_{1,ij}$, $\alpha_{2,ij}$, $\alpha_{3,ij}$, $\alpha_{4,ij}$, and $\alpha_{5,ij}$ are obtained to calculate the values of $a_{10\ 01}$, $i = 10$ and $j = 01$ (10th row and 1st column)

$$\alpha_{1,10\ 01} = -0.0523, \ \alpha_{2,10\ 01} = 0.1054,$$
$$\alpha_{3,10\ 01} = 0.0513, \ \alpha_{4,10\ 01} = -0.0039,$$
$$\alpha_{5,10\ 01} = 0.0146$$

From equation (7)

$$a_{10\ 01} = -0.0523e^{-20\times0.31} + 0.1054e^{-15\times0.31}$$
$$+ 0.0513e^{-8\times0.31} - 0.0039e^{-2.5\times0.31} + 0.0146$$
$$a_{10\ 01} = 0.0180$$

Similarly, the other values $(a_{10\ 02}, a_{10\ 03}, \ldots, a_{10\ 10})$ can be determined using the corresponding coefficients

$$a_{10\ 02} = 0.0171, \ a_{10\ 03} = 0.0160,$$
$$a_{10\ 04} = 0.0150, \ a_{10\ 05} = 0.0139$$
$$a_{10\ 06} = 0.0127, \ a_{10\ 07} = 0.0114,$$
$$a_{10\ 08} = 0.0101, \ a_{10\ 09} = 0.0088, \ a_{10\ 10} = 0.0071$$

From Supplemental Appendix, Tables 16–20, the equation coefficients $\beta_{1,ij}$, $\beta_{2,ij}$, $\beta_{3,ij}$, $\beta_{4,ij}$, and $\beta_{5,ij}$ are obtained, and the coefficients of the $\bar{b}$ matrix can be determined

$$b_{10\ 01} = 0.0280, \ b_{10\ 02} = 0.0274,$$
$$b_{10\ 03} = 0.0265, \ b_{10\ 04} = 0.0254, \ b_{10\ 05} = 0.0241$$
$$b_{10\ 06} = 0.0226, \ b_{10\ 07} = 0.0209, \ b_{10\ 08} = 0.0190,$$
$$b_{10\ 09} = 0.0169, \ b_{1010} = 0.0142$$

The above coefficients are for hole diameter $D_0 = 2\,\text{mm}$. From equation (9), the coefficient $a_{10\ 01}$ for the effective hole diameter can be computed as

$$a_{10\ 01} = 0.0180 \times 1.79^2/2^2 = 0.0144$$

and the following are the final coefficients to be used

$$a_{10\ 01} = 0.0144, \ a_{10\ 02} = 0.0136, \ a_{10\ 03} = 0.0128,$$
$$a_{10\ 04} = 0.0120, \ a_{10\ 05} = 0.0111$$
$$a_{10\ 06} = 0.0102, \ a_{10\ 07} = 0.0092, \ a_{10\ 08} = 0.0081,$$
$$a_{10\ 09} = 0.0070, \ a_{10\ 10} = 0.0057$$
$$b_{10\ 01} = 0.0225, \ b_{10\ 02} = 0.0219, \ b_{10\ 03} = 0.0212,$$
$$b_{10\ 04} = 0.0204, \ b_{10\ 05} = 0.0193$$
$$b_{10\ 06} = 0.0181, \ b_{10\ 07} = 0.0167, \ b_{10\ 08} = 0.0152,$$
$$b_{10\ 09} = 0.0135, \ b_{10\ 10} = 0.0113$$